

Observation of Elusive $\text{CF}_2\text{Cl}\cdots\text{Cl}$ in Matrix Infrared Spectra and Density Functional Calculations

Han-Gook Cho

Department of Chemistry, University of Incheon, Incheon 406-772, Korea. E-mail: hgc@incheon.ac.kr
Received August 7, 2013, Accepted August 15, 2013

$\text{CF}_2\text{Cl}\cdots\text{Cl}$, an elusive photo-isomer of CF_2Cl_2 , has been observed in matrix IR spectra from the precursors exposed to radiation from laser ablation of transition-metals. Other plausible products, $\text{CFCl}_2\cdots\text{F}$ and $\text{FCIC}\cdots\text{F-Cl}$ are not detected due to their considerably higher energies. Parallel to its previously reported analogues, the C-X bonds are considerably stronger than those of the reactant, and particularly the Cl atom that is weakly bound to the residual Cl atom forms an unusually strong carbon-halogen bond. NBO analysis reveals that the C-Cl bond is a true double bond, and the weak $\text{Cl}\cdots\text{Cl}$ bond is largely ionic, $\text{F}_2\text{C}=\text{Cl}^{\delta+}\cdots\text{Cl}^{\delta-}$. IRC computation reproduces smooth inter-conversion between the reactant and product, and the transition state is energetically close to the product, consistent with its prompt disappearance in the early stage of photolysis.

Key Words : *iso*-Halomethane, Infrared, DFT, Matrix, Laser-ablation

Introduction

Halomethanes not only cause ozone depletion in the stratosphere, but also are strong, long-lasting greenhouse gases.^{1,2} The fragments (radicals, ions) and isomers of halomethanes are reaction intermediates of many atmospheric reactions. Therefore, the spectroscopic properties of these unstable species are important to understand the photo-reactions and other behaviors of the environmentally hazardous halogen-containing gases.³⁻⁵

The unstable *iso*-tetrachloromethane $\text{CCl}_3\cdots\text{Cl}$ was first identified by Maier and coworkers following selective irradiation in the photo-dissociation region (222 nm through 193 nm) for CCl_4 in solid argon.^{6a} Later work of Jacox *et al.* produced related chlorocarbon ions and the $\text{CCl}_3\cdots\text{Cl}$ species in solid neon.^{6b} The $\text{CH}_2\text{X}\cdots\text{X}$ (X = Cl, Br, I) species were also detected by Maier *et al.* via photo-isomerization of methylene halides, and the structures and vibrational frequencies were computed using MP2 methods.^{7a} The infrared absorptions of these species with a weak $\text{X}\cdots\text{X}$ bond disappear on visible irradiation in the early stage of photolysis, indicating that they are shallow energy minima.^{6,7}

$\text{CHCl}_2\cdots\text{Cl}$, $\text{CHFCI}\cdots\text{Cl}$, $\text{CHBr}_2\cdots\text{Br}$, and $\text{CFCl}_2\cdots\text{Cl}$ have recently been observed in the matrix IR spectra via photo-isomerization of their precursors during co-deposition of laser-ablated transition-metal atoms.⁸ $\text{CBr}_3\cdots\text{Br}$ was detected in radiolysis experiment.⁹ NBO analysis¹⁰ reveal that the C-X bond is a true double bond and the weak $\text{X}\cdots\text{X}$ bond is largely ionic, $\text{X}_2\text{C}=\text{X}^{\delta+}\cdots\text{X}^{\delta-}$ (X = H, halogen). The fluorine-containing *iso*-halomethanes are rare. No *iso*-halomethanes with an $\text{F}\cdots\text{F}$, $\text{F}\cdots\text{Cl}$, or $\text{Cl}\cdots\text{F}$ bond have been identified, and moreover, no *iso*-halomethanes with two F atoms and an $\text{X}\cdots\text{X}$ bond have been reported to date.

Recently a new breed of small high oxidation-state transition-metal complexes are produced in reactions with halomethanes.^{11,12} Along with the metal containing products,

photo-reaction products of the precursor (radicals, ions, and isomers) are also observed in the matrix spectra, due to the plume radiation from laser ablation. In this paper, we report observation of elusive $\text{CF}_2\text{Cl}\cdots\text{Cl}$ with ^{13}C shifts for comparison. DFT and intrinsic reaction coordinate computations¹³ reveal smooth inter-conversion between the reactant and product, and the transition state is energetically close to the product, consistent with the disappearance of the product in the early stage of photolysis.

Experimental

The $\text{CF}_2\text{Cl}\cdots\text{Cl}$ photo-isomer spectra shown in this report were recorded from samples prepared by co-deposition of laser-ablated Hf atoms with CF_2Cl_2 and $^{13}\text{CF}_2\text{Cl}_2$ (Dupont) in excess argon at 10 K using a closed-cycle refrigerator (Air Products, Displex). While the product absorptions are strongest in the Hf spectra, other metals (groups 3-11 and actinides) also yield the same product absorptions although the intensities vary owing to different laser ablation plume radiation from specific metal surfaces.^{11,12} Hence, these metal independent absorptions do not arise from metal containing species

In this study, Hf atoms and intense radiation from the laser ablation plume impinge on the depositing matrix sample. These methods have been described in detail elsewhere.¹⁴ Reagent gas mixtures are typically 0.50% in argon. The Nd:YAG laser fundamental (1064 nm, 10 Hz repetition rate, 10 ns pulse width) was focused onto the rotating metal target (Johnson-Matthey) using 5-10 mJ/pulse. After co-deposition, infrared spectra were recorded at 0.5 cm^{-1} resolution using a Nicolet 550 spectrometer with a Hg-Cd-Te range B detector. Then samples were irradiated for 20 min periods by a mercury arc street lamp (175 W) with the globe removed using a combination of optical filters or annealed to allow further reagent diffusion.

Complementary density functional theory (DFT) calculations were carried out using the Gaussian 09 package,¹⁵ the B3LYP density functional,¹⁶ and 6-311++G(3df,3pd) basis sets for C, F, and Cl to provide a consistent set of vibrational frequencies and energies for the reaction products and their analogues. Geometries were fully relaxed during optimization, and the optimized geometry was confirmed by vibrational analysis. Additional BPW91¹⁷ calculations were done to confirm the B3LYP results. The vibrational frequencies were calculated analytically, and the zero-point energy is included in the calculation of binding energy of a metal complex. Intrinsic reaction coordinate (IRC) calculations¹³ have been performed to link the transition state structures with the reactants and specific products.

Results and Discussion

$\text{CF}_2\text{Cl}\cdots\text{Cl}$ Absorptions. Figure 1 shows the $\text{CF}_2\text{Cl}\cdots\text{Cl}$ absorption region for CF_2Cl_2 co-deposited with laser-ablated Hf atoms. The product absorptions marked “t” are observed in the original deposition spectra, but disappear in concert upon subsequent irradiation with $\lambda > 290$ nm. They do not reappear in the following full arc ($\lambda > 220$ nm) photolysis and annealing to 30 K. The early disappearance of these product absorptions in the process of photolysis is in line with those of the previously reported *iso*-halomethanes.⁶⁻⁸ The weak absorption intensities shown in Figure 1 are consistent with the rarity of F containing halomethane photoisomers; $\text{CHFCl}\cdots\text{Cl}$ and $\text{CFCl}_2\cdots\text{Cl}$ are the only fluorine containing *iso*-halomethanes reported to date.

New product absorptions are observed at 1281 and 1256 cm^{-1} with intensity ratio of $\sim 1:2.5$ on the blue side of the CF_2 stretching absorptions of the precursor at 1150 and 1090 cm^{-1} . The frequencies are also compared with the previously reported C-F stretching frequencies of 1199 and 1211 cm^{-1} for CHFClCl and CFCl_2Cl .⁸ They shift to 1250 and 1219 cm^{-1} on ^{13}C substitution (12/13 ratios of 1.025 and 1.030). No other considerable product absorptions are observed. The observed vibrational characteristics do not match with the previously reported values for the fragments (ions and radicals) of CF_2Cl_2 .³⁻⁵ They are assigned to the anti-sym-

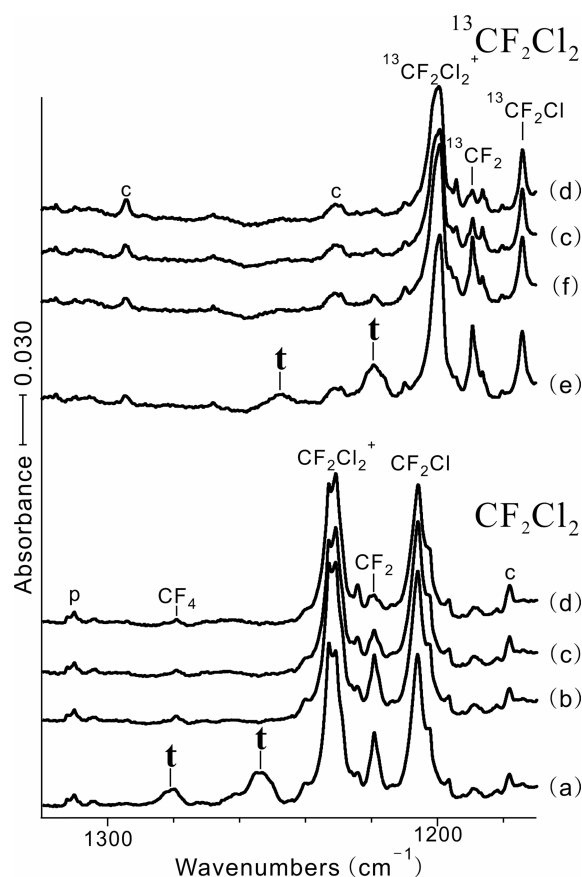


Figure 1. IR spectra for the $\text{CF}_2\text{Cl}\cdots\text{Cl}$ absorptions produced from CF_2Cl_2 co-deposited for 1 h with laser-ablated Hf atoms in excess argon at 10 K and their variation. (a) Hf + 0.50% CF_2Cl_2 co-deposited for 1 h and (b)–(d) as (a) after irradiation with $\lambda > 290$ and $\lambda > 220$ nm and annealing to 30 K. (e) Hf + 0.50% $^{13}\text{CF}_2\text{Cl}_2$ co-deposited for 1 h and (f)–(h) as (a) after irradiation with $\lambda > 290$ and $\lambda > 220$ nm and annealing to 30 K. t indicates the $\text{CF}_2\text{Cl}\cdots\text{Cl}$ absorptions, and p and c designate precursor and common absorptions. The absorptions of the CF_2Cl_2^+ and CFCl_2 are also indicated.

metric and symmetric CF_2 stretching modes of $\text{CF}_2\text{Cl}\cdots\text{Cl}$ on the basis of their frequencies, relatively large ^{13}C shifts, and good correlation with the predicted values. The computed frequencies are 1302 and 1286 cm^{-1} , ^{13}C shifts both 36

Table 1. Observed and DFT Fundamental Frequencies of $\text{CF}_2\text{Cl}\cdots\text{Cl}$ Isotopomers in the Ground $^1\text{A}'$ Electronic State^a

Approximate Description	$\text{CF}_2\text{Cl}\cdots\text{Cl}$					$^{13}\text{CF}_2\text{Cl}\cdots\text{Cl}$				
	Obs	B3LYP ^b	Int ^b	BPW91 ^c	int ^c	Obs	B3LYP ^b	Int ^b	BPW91 ^c	int ^c
A" as CF_2 str.	1281	1302	276	1231	266	1250	1266	259	1197	250
A' s CF_2 str.	1256	1286	647	1224	553	1219	1250	612	1189	523
A' C-Cl str.		734	35	697	27		731	33	693	25
A' CCl_2F deform		544	15	529	20		532	8	516	13
A' CF_2 scis.		446	93	435	74		440	94	431	77
A" CF_2 rock		411	1	392	0		409	1	390	0
A' Cl-Cl str.		256	87	259	64		256	88	259	64
A" CClCl oop bend		126	2	125	1		126	2	125	1
A' CClCl ip bend		85	9	90	7		85	9	90	7

^aFrequencies observed in solid argon in recent laser ablation experiments; bold are stronger matrix sites. Harmonic frequencies (cm^{-1}) and intensities (km/mol) were computed with 6-311++G(3df,3pd). ^bComputed with B3LYP. ^cComputed with BPW91.

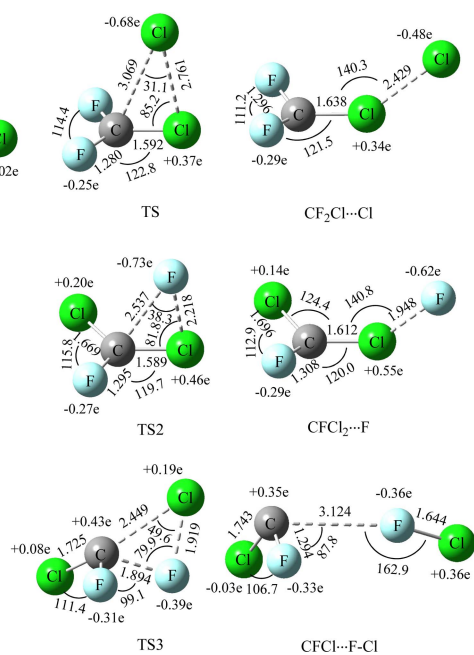


Figure 2. The B3LYP structures of CF_2Cl_2 , the transition states, and the plausible products ($\text{CF}_2\text{Cl}\cdots\text{Cl}$, $\text{CFCl}_2\cdots\text{F}$, and $\text{FCIC}\cdots\text{F-Cl}$). The bond lengths and angles are in Å and degrees. The natural atomic charges are also shown. Only $\text{CF}_2\text{Cl}\cdots\text{Cl}$ is observed in this study (see text).

cm^{-1} , and intensity ratio between the two bands 1:2.3 (Table 1). These two are the strongest bands of the photo-isomer, and the other bands are too weak to observe. The observed product absorptions and isotopic shifts support formation of the first *iso*-halomethane containing two F atoms ($\text{CF}_2\text{Cl}\cdots\text{Cl}$).

$\text{CFCl}_2\cdots\text{F}$ and $\text{FCIC}\cdots\text{F-Cl}$, other plausible products, are not detected. $\text{CFCl}_2\cdots\text{F}$ would show its strong C-F and C-Cl stretching absorptions at ~ 1200 and 1020 cm^{-1} , which are not observed. The strongest C-F and C-Cl stretching absorptions of $\text{FCIC}\cdots\text{F-Cl}$ expected at ~ 1140 and 710 cm^{-1} are also not observed. $\text{CF}_2\text{Cl}\cdots\text{Cl}$, $\text{CFCl}_2\cdots\text{F}$, and $\text{FCIC}\cdots\text{F-Cl}$ are 251, 321, and 446 kJ/mol higher than the precursor. On the contrary, the attempts to optimize the geometry of $\text{Cl}_2\text{C}\cdots\text{F-F}$ all ended up with the structure of CF_2Cl_2 , suggesting that the *iso*-tetrahalomethane with an F-F bond is not a

meaningful energy minimum. Clearly, the observed photo-isomer of CF_2Cl_2 with a $\text{Cl}\cdots\text{Cl}$ bond is the most stable.

Molecular Structures and Bonding. Figure 2 shows the B3LYP structures of the precursor (CF_2Cl_2), transition states, and plausible three *iso*-tetrahalomethanes ($\text{CF}_2\text{Cl}\cdots\text{Cl}$ and $\text{CFCl}_2\cdots\text{F}$, and $\text{FCIC}\cdots\text{F-Cl}$). The C and three atoms bonded to C form a near planar structure with a bridging halogen atom in the transition state. The product structure is in fact similar to that of the transition state, other than the larger $\langle\text{CXX}\rangle$, indicating that the transition state is energetically closer to the product than the reactant. The C-X bond lengths of the products are considerably shorter than those of the precursor. The C-F and C-Cl bond lengths of 1.296 and 1.638 Å for $\text{CF}_2\text{Cl}\cdots\text{Cl}$ and 1.308 and 1.696 and 1.612 Å for $\text{CFCl}_2\cdots\text{F}$ are compared with those of 1.332 and 1.772 Å for the CF_2Cl_2 . Particularly the Cl atom bonded to the residual X atom forms an exceptionally strong bond with carbon (C-Cl bond lengths of 1.638 and 1.612 Å in $\text{CF}_2\text{Cl}\cdots\text{Cl}$ and $\text{CFCl}_2\cdots\text{F}$). On the other hand, The $\text{Cl}\cdots\text{Cl}$ and $\text{Cl}\cdots\text{F}$ bond lengths (2.429 and 1.948 Å) are significantly longer than those of Cl_2 and FCl (2.011 and 1.643 Å) computed at the same level of theory.

The Natural atomic charges, bond lengths, occupancies, bond orders,¹⁰ and structural parameters of $\text{CF}_2\text{Cl}\cdots\text{Cl}$ and $\text{CFCl}_2\cdots\text{F}$ are listed in Table 2 with those of several previously reported *iso*-halomethanes.⁸ The unusually short C-X bonds have considerable double bond character (natural bond orders of 1.549 and 1.648 for $\text{CF}_2\text{Cl}\cdots\text{Cl}$ and $\text{CFCl}_2\cdots\text{F}$). The $\text{Cl}\cdots\text{X}$ bond is largely ionic (natural atomic charges of 0.339 and -0.477 for $\text{CF}_2\text{Cl}\cdots\text{Cl}$ and those of 0.548 and -0.618 for $\text{CFCl}_2\cdots\text{F}$). Hence, these photo-isomers are better represented as $\text{X}_2\text{C}=\text{X}^{\delta+}\cdots\text{X}^{\delta-}$. Similarly, in the structure of transition state, the bridging X carries a substantial amount of negative charge, indicating that it is largely ionically bonded to the planar CX_3 subunit. The bridging Cl and F in the transition states in the $\text{CF}_2\text{Cl}_2 \leftrightarrow \text{CF}_2\text{Cl}\cdots\text{Cl}$ and $\text{CF}_2\text{Cl}_2 \leftrightarrow \text{CFCl}_2\cdots\text{F}$ conversions own natural atomic charges of -0.681 and -0.728 , $[\text{CF}_2\text{Cl}]^{0.681+}\cdots\text{Cl}^{0.681-}$ and $[\text{CFCl}_2]^{0.728+}\cdots\text{F}^{0.728-}$.

The structure of $\text{FCIC}\cdots\text{F-Cl}$, which is much higher in energy than $\text{CF}_2\text{Cl}\cdots\text{Cl}$ and $\text{CFCl}_2\cdots\text{F}$, is also shown in Figure 2. F cannot expand its valency unlike Cl, which can

Table 2. Natural Atomic Charges, Bond Lengths, Occupancies, Natural Bond Orders and Structural Parameters of the *iso*-halomethanes with weak Halogen-Halogen Bonds Investigated in this Study^a

Compound	Q_1^b	Q_2^b	Q_3^b	Q_4^b	Q_5^b	$r(\text{C}=\text{X})^c$	Occ (C=X) ^d	BO (C=X) ^d	$r(\text{X}^{\delta+}\cdots\text{X}^{\delta-})^e$	$\langle\text{CXX}\rangle^e$	$\Phi(\text{HXCX})^f$
$\text{F}_2\text{C}=\text{Cl}^{\delta+}\cdots\text{Cl}^{\delta-}$	-0.291	-0.291	0.720	0.339	-0.477	1.638	1.809, 1.289	1.549	2.429	140.3	153.0
$\text{FCIC}=\text{Cl}^{\delta+}\cdots\text{F}^{\delta-}$	-0.299	0.136	0.234	0.548	-0.618	1.612	1.849, 1.446	1.648	1.948	140.8	162.3
$\text{H}_2\text{C}=\text{Cl}^{\delta+}\cdots\text{Cl}^{\delta-}$	0.197	0.197	-0.383	0.436	-0.448	1.600	1.932, 1.535	1.733	2.435	122.1	165.9
$\text{HCIC}=\text{Cl}^{\delta+}\cdots\text{Cl}^{\delta-}$	0.209	0.134	-0.312	0.445	-0.476	1.606	1.924, 1.371	1.648	2.473	125.0	164.1
$\text{HFC}=\text{Cl}^{\delta+}\cdots\text{Cl}^{\delta-}$	0.179	-0.293	0.196	0.408	-0.490	1.598	1.882, 1.460	1.671	2.467	126.9	162.0
$\text{FCIC}=\text{Cl}^{\delta+}\cdots\text{Cl}^{\delta-}$	-0.298	0.148	0.230	0.412	-0.493	1.619	1.876, 1.304	1.590	2.470	133.2	159.1
$\text{Cl}_2\text{C}=\text{Cl}^{\delta+}\cdots\text{Cl}^{\delta-}$	0.164	0.164	-0.290	0.450	-0.487	1.619	1.893, 1.253	1.572	2.487	128.8	164.4

^aComputed with B3LYP/6-311++G(3df, 3pd). The all electron basis is used for H, C, F, and Cl. ^bNatural atomic charges in the order in the molecular formula. For example, H, Cl, C, Cl, and Cl are atom 1, 2, 3, 4, and 5 for $\text{HCIC}=\text{Cl}^{\delta+}\cdots\text{Cl}^{\delta-}$. ^cThe unusually short C-X bondlength. ^dNatural occupancies of σ and π orbitals of the C=X bond and its bond order. ^eX-X bondlength and CXX angle. ^fDihedral angle of $\text{X}_1\text{X}_2\text{C}=\text{X}_4$ structure.

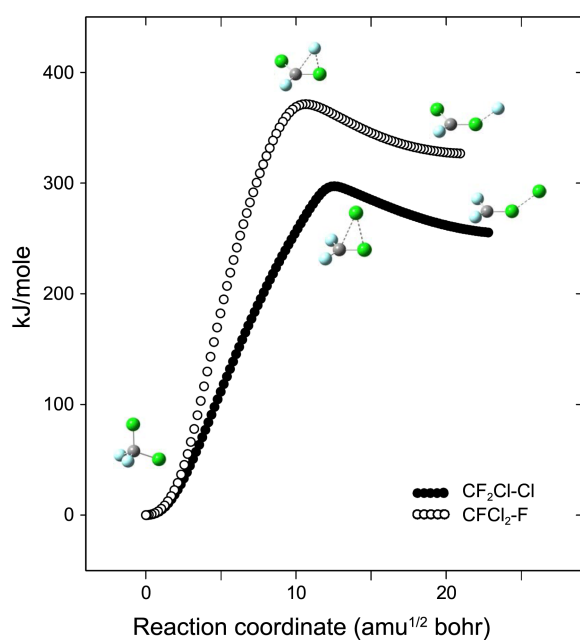


Figure 3. Intrinsic reaction coordinate (IRC) calculations between CF_2Cl_2 and $CF_2Cl\cdots Cl$ and between CF_2Cl_2 and $CFCl_2\cdots F$. The shallow energy minimum for $CF_2Cl\cdots Cl$ leads to prompt conversion of the transient species to CF_2Cl_2 . $CFCl_2\cdots F$ is not observed in this study due to its high energy.

utilize its 3d-orbitals. During geometry optimization, the initial geometry of $CFClF\cdots Cl$ converges to the structure of $FCIC\cdots F-Cl$. The F-Cl bondlength of 1.644 Å in $CFCl\cdots F-Cl$ is essentially the same as that of 1.643 Å for F-Cl calculated at the same level of theory, and the interatomic distance between C and F is 3.124 Å as shown in Figure 2.

Reactions. Intrinsic reaction coordinate¹³ (IRC) computations are carried out for the isomerization reactions between CF_2Cl_2 and the plausible products. Figure 3 shows the IRC results for the $CF_2Cl_2 \leftrightarrow CF_2Cl\cdots Cl$ and $CF_2Cl_2 \leftrightarrow CFCl_2\cdots F$ systems. Due to the large energy difference between the reactant and product, the transition state is energetically much closer to the product. The activation energies from the reactant to CF_2Cl-Cl and $CFCl_2-F$ (294 and 365 kJ/mol) are noticeably higher than those for previously introduced $CHCl_2\cdots Cl$, $CHFCl\cdots Cl$, $CFCl_2\cdots Cl$, and $CCl_3\cdots Cl$ (248, 274, 254, and 220 kJ/mol, respectively).⁸ Fluorine evidently increases the activation energy from the precursor to the *iso*-halomethane, and the high activation energy is consistent with the observed weak product absorptions (the low yield) of $CF_2Cl\cdots Cl$. The activation energy from CF_3Cl to $CF_2Cl\cdots F$ is even higher (406 kJ/mol), consistent with its absence in the CF_3Cl spectra.¹⁸

In contrast, the activation energies in the reverse reactions are considerably smaller (43 and 44 kJ/mol, respectively), consistent with the disappearance of the product in the early stage of photolysis. Separate IRC computation has also been carried out for production of $FCIC\cdots F-Cl$, showing that its transition state, which is 555 kJ/mol higher than the reactant, is also linked smoothly to the reactant and product. Evidently the high energy barrier prohibits production of $FCIC\cdots F-$

Cl as well as $CFCl_2\cdots F$.

Conclusion

$CF_2Cl\cdots Cl$, the first *iso*-halomethane with two F atoms, is produced from CF_2Cl_2 during co-deposition with laser-ablated metal atoms and the associated laser plume irradiation and identified in the matrix IR spectra with isotopic substitution and DFT computational results. The absorptions of this photo-isomer are relatively weak, and they disappear in the early stage of photolysis, parallel to those of its analogues from di-, tri-, and tetra-halomethanes. The other plausible products, $CFCl_2\cdots F$ and $FCIC\cdots F-Cl$, are not identified due to their considerably higher energies. $Cl_2C\cdots F-F$ is probably not a meaningful energy minimum.

$CF_2Cl\cdots Cl$ has a near planar structure of the C and three atoms bonded to C, and the residual X atom is bonded to the Cl atom. The product structure is similar to the structure of the transition state except for the larger $\angle CXX$. The C-X bonds of the product are considerably stronger than those of the precursor. Particularly the Cl atom that is bonded to the residual X atom forms an unusually strong C-Cl bond. NBO analysis reveals that the strong carbon-chlorine bond has considerable double bond character (natural bond order >1.5). The weak $Cl\cdots X$ bond is largely ionic on the basis of the large atomic charges, $X_2C=Cl^{\delta+}\cdots X^{\delta-}$.

The IRC calculations reproduce smooth conversion between the reactant and product. The transition state is much closer in energy to the product, consistent with the disappearance of the product in the early stage of photolysis and the similarity in the structures of the transition state and product. The previous and present results show that the activation energy to the *iso*-halomethane increases substantially with the number of F, making formation of the photo-isomer increasingly difficult.

Acknowledgments. This work is supported by University of Incheon Research Grant in 2011.

References

- (a) Barrie, L. A.; Bottenheim, J. W.; Schnell, R. C.; Crutzen, P. I.; Rasmussen, R. A. *Nature* **1988**, *334*, 138-141. (b) Dix, B.; Baidar, S.; Bresch, J. F.; Hall, S. R.; Schmidt, K. S.; Wang, S.; Volkamer, R. *PNAS* **2013**, *110*, 2035-2040. (c) Newman, P. A.; Daniel, J. S.; Waugh, D. W.; Nash, E. R. *Atmos. Chem. Phys.* **2007**, *7*, 4537-4552. (d) Toon, O. B.; Turco, R. P. *Sci. Am.* **1991**, *264*, 6, 68-74.
- (a) Ashford, P.; Clodic, D.; McCulloch, A.; Kuijpers, L. *Int. J. Refrig.* **2004**, *27*, 687-700. (b) Keller, C. A.; Hill, M.; Voller, M. K.; Henne, S.; Brunner, D.; Reimann, S.; O'Doherty, S.; Arduini, J.; Maione, M.; Ferenczi, Z. *et al. Environ. Sci. Technol.* **2012**, *46*, 217-225. (c) Akiyoshi, H.; Yamashita, Y.; Sakamoto, K.; Zhou, L. B.; Imamura, T. *J. Geophys. Res.* **2010**, *115*, D19301, 1-22. (d) Karl, T. R.; Trenberth, K. E. *Science* **2003**, *302*, 1719-1723.
- (a) Dearden, D. V.; Hudgens, J. W.; Johnson, R. D., III; Tsai, B. P.; Kafafi, S. A. *J. Phys. Chem.* **1992**, *96*, 585-594. (b) Vogelhuber, K. M.; Wren, S. W.; McCoy, A. B.; Ervin, K. M.; Lineberger, W. C. *J. Chem. Phys.* **2011**, *134*, 184306, 1-13. (c) Andrews, L.; Dyke, J. M.; Jonathan, N.; Keddar, N.; Morris, A. *J. Am. Chem.*

- Soc.* **1984**, *106*, 299-303. (d) Carver, T. G.; Andrews, L. *J. Chem. Phys.* **1969**, *50*, 4235-4245.
4. (a) Guss, J. S.; Votava, O.; Kable, S. H. *J. Chem. Phys.* **2001**, *115*, 11118-11130. (b) Schiachta, R.; Lask, G. M.; Bondybey, V. E. *Faraday Trans.* **1991**, *87*, 2407-2412. (c) Milligan, D. E.; Jacox, M. E. *J. Chem. Phys.* **1967**, *47*, 703-707. (d) Prochaska, F. T.; Andrews, L. *J. Chem. Phys.* **1978**, *68*, 5568-5576.
5. Jacox, M. E. *J. Phys. Chem. Ref. Data* **2003**, *32*, 1-441, and references therein.
6. (a) Maier, G.; Reisenauer, H. P.; Hu, J.; Hess, B. A., Jr.; Schaad, L. J. *Tetrahed. Lett.* **1989**, *30*, 4105-4108. (b) Lugez, C. L.; Jacox, M. E.; Johnson, R. D., III. *J. Chem. Phys.* **1998**, *109*, 7147-7156 and references therein. (c) Herzberg, G. *Infrared and Raman Spectra*; Van Nostrand: Princeton, 1945.
7. (a) Maier, G.; Reisenauer, H. P.; Hu, J.; Schaad, L. J.; Hess, B. A., Jr. *J. Am. Chem. Soc.* **1990**, *112*, 5117-5122. (b) Andrews, L.; Prochaska, F. T.; Ault, B. S. *J. Am. Chem. Soc.* **1979**, *101*, 9-15. (c) Cho, H.-G.; Andrews, L. *Organometallics* **2009**, *28*, 1358-1368. (d) Andrews, L.; Smith, D. W. *J. Chem. Phys.* **1970**, *53*, 2956-2966. (e) Andrews, L.; Dyke, J. M.; Jonathan, N.; Keddar, N.; Morris, A. *J. Am. Chem. Soc.* **1984**, *106*, 299-303.
8. Cho, H.-G.; Andrews, L. *J. Phys. Chem. A* **2013**, *117*, 6525-6535.
9. (a) Andrews, L.; Grzybowski, J. M.; Allen, R. O. *J. Phys. Chem.* **1975**, *79*, 905-912. (b) Prochaska, F. T.; Andrews, L. *J. Chem. Phys.* **1977**, *67*, 1091-1098 and references therein. (c) Andrews, L.; Prochaska, F. T. *J. Phys. Chem.* **1979**, *83*, 368-372. (d) Machara, N. P.; Ault, B. S. *J. Chem. Phys.* **1988**, *88*, 2845-2846.
10. Reed, A. E.; Curtiss, L. A.; Weinhold, F. *Chem. Rev.* **1988**, *88*, 899-926, and references therein.
11. (a) Andrews, L.; Cho, H.-G. *Organometallics* **2006**, *25*, 4040-4053, and references therein. (Review article). (b) Cho, H.-G.; Andrews, L. *Eur. J. Inorg. Chem.* **2008**, 2537-2549. (c) Cho, H.-G.; Andrews, L. *Organometallics* **2010**, *29*, 2211-2222. (d) Cho, H.-G.; Andrews, L. *Dalton Trans.* **2010**, *39*, 5478-5489. (e) Cho, H.-G.; Andrews, L. *Organometallics* **2011**, *30*, 477-486.
12. (a) Lyon, J. T.; Andrews, L. *Organometallics* **2007**, *26*, 4152-4159. (b) Cho, H.-G.; Andrews, L. *Dalton Trans.* **2009**, 5858-5866.
13. Fukui, K. *Acc. Chem. Res.* **1981**, *14*, 363-368.
14. (a) Andrews, L.; Citra, A. *Chem. Rev.* **2002**, *102*, 885-911, and references therein. (b) Andrews, L. *Chem. Soc. Rev.* **2004**, *33*, 123-132, and references therein.
15. Frisch, M. J.; Trucks, G. W.; Schlegel, H. B.; Scuseria, G. E.; Robb, M. A.; Cheeseman, J. R.; Scalmani, G.; Barone, V.; Mennucci, B.; Petersson, G. A. *et al.* Gaussian 09, revision A.02; Gaussian, Inc.: Wallingford, CT, 2009.
16. (a) Becke, A. D. *J. Chem. Phys.* **1993**, *98*, 5648-5653. (b) Lee, C.; Yang, Y.; Parr, R. G. *Phys. Rev. B* **1988**, *37*, 785-789.
17. Burke, K.; Perdew, J. P.; Wang, Y. In *Electronic Density Functional Theory: Recent Progress and New Directions*; Dobson, J. F., Vignale, G., Das, M. P., Eds.; Plenum: 1998.
18. Cho, H.-G.; Andrews, L. *J. Am. Chem. Soc.* **2008**, *130*, 15836-15841.
-